SMC-TR-95-36

Fracture in MoS2 Solid Lubricant Films

1 September 1995

Prepared by

M. R. HILTON
Mechanics and Materials Technology Center
Technology Operations

Prepared for

SPACE AND MISSILE SYSTEMS CENTER
AIR FORCE MATERIEL COMMAND
2430 E. El Segundo Boulevard
Los Angeles Air Force Base, CA 90245

DTIC
SELECTED
NOV 06 1995
B

Engineering and Technology Group

19951103 018

DTIC QUALITY INSPECTED 1

THE AEROSPACE
CORPORATION
El Segundo, California

This report has been reviewed by the Public Affairs Office (PAS) and is releasable to the National Technical Information Service (NTIS). At NTIS, it will be available to the general public, including foreign nationals.

This technical report has been reviewed and is approved for publication. Publication of this report does not constitute Air Force approval of the report's findings or conclusions. It is published only for the exchange and stimulation of ideas.

H. KEVIN PSMITHE, CAPT, USAF
Space Environmental Sensor Team Chief
Defense Meteorological Satellite Program

REPORT DOCUMENTATION PAGE

Public reporting burden for this collection of information is estimated to average 1 hour per response, including the time for reviewing instructions, searching existing data sources, gathering and maintaining the data needed, and completing and reviewing the collection of information. Send comments regarding this burden estimate or any other aspect of this collection of information, including suggestions for reducing this burden to Washington Headquarters Services, Directorate for Information Operations and Reports, 1215 Jefferson Davis Highway, Suite 1204, Arlington, VA 22202-4302, and to the Office of Management and Budget, Paperwork Reduction Project (0704-0188), Washington, DC 20503.

1. AGENCY USE ONLY (Leave blank)	2. REPORT DATE	3. REPORT TYPE AND DATES COVERED

4. TITLE AND SUBTITLE

Fracture in MoS_2 Solid Lubricant Films

5. FUNDING NUMBERS

F04701-93-C-0094

6. AUTHOR(S)

Hilton, Michael R.

7. PERFORMING ORGANIZATION NAME(S) AND ADDRESS(ES)

The Aerospace Corporation
Technology Operations
El Segundo, CA 90245-4691

8. PERFORMING ORGANIZATION REPORT NUMBER

TR-94(4935)-6

9. SPONSORING/MONITORING AGENCY NAME(S) AND ADDRESS(ES)

Space and Missile Systems Center
Air Force Materiel Command
2430 E. El Segundo Blvd.
Los Angeles Air Force Base, CA 90245

10. SPONSORING/MONITORING AGENCY REPORT NUMBER

SMC-TR-95-36

11. SUPPLEMENTARY NOTES

12a. DISTRIBUTION/AVAILABILITY STATEMENT

Approved for public release; distribution unlimited

12b. DISTRIBUTION CODE

13. ABSTRACT (Maximum 200 words)

The fracture properties of sputter-deposited films of MoS_2 as a function of the additive-controlled microstructure were assessed using brale indentation contact and scanning electron microscopy (SEM). Additives were incorporated as either co-sputtered species (Ni, SbO_x or as multilayers (Au–20%Pd, Ni). Undoped films were also examined as references. The undoped films and 3% co-sputtered Ni films (deposited at 2.66 Pa argon background pressure) showed zone 2 columnar plate morphologies with porosity. Co-sputtered films having higher concentratons of Ni or SbO_x showed zone 1 dense cauliflower morphologies, while the multilayer films (and pure MoS_2 films deposited at 0.266 Pa) exhibited dense, featureless morphologies. The porous zone 2 films generally resisted delamination better than the denser morphologies. High Ni concentrations increased spallation. The presence of SbO_x affected fracture propagation and appeared to be more benign than Ni. The presence of multilayers also affected fracture and retarded spallation in dense microstructures. However, many multilayer structures showed significant delamination.

14. SUBJECT TERMS

Bearings
MoS_2
Indentation testing
Solid lubricants

15. NUMBER OF PAGES

13

16. PRICE CODE

17. SECURITY CLASSIFICATION OF REPORT	18. SECURITY CLASSIFICATION OF THIS PAGE	19. SECURITY CLASSIFICATION OF ABSTRACT	20. LIMITATION OF ABSTRACT
Unclassified	Unclassified	Unclassified	

NSN 7540-01-280-5500

Standard Form 298 (Rev. 2-89)
Prescribed by ANSI Std. Z39-18
298-102

Fracture in MoS_2 solid lubricant films

Michael R. Hilton

Mechanics and Materials Technology Center, The Aerospace Corporation, El Segundo, CA 90245, USA

Abstract

The fracture properties of sputter-deposited films of MoS_2 as a function of the additive-controlled microstructure were assessed using brale indentation contact and scanning electron microscopy (SEM). Additives were incorporated as either co-sputtered species (Ni, SbO_x) or as multilayers (Au–20%Pd, Ni). Undoped films were also examined as references. The undoped films and 3% co-sputtered Ni films (deposited at 2.66 Pa argon background pressure) showed zone 2 columnar plate morphologies with porosity. Co-sputtered films having higher concentrations of Ni or SbO_x showed zone 1 dense cauliflower morphologies, while the multilayer films (and pure MoS_2 films deposited at 0.266 Pa) exhibited dense, featureless morphologies. The porous zone 2 films generally resisted delamination better than the denser morphologies. High Ni concentrations increased spallation. The presence of SbO_x affected fracture propagation and appeared to be more benign than Ni. The presence of multilayers also affected fracture and retarded spallation in dense microstructures. However, many multilayer structures showed significant delamination.

1. Introduction

Since the earliest reports of sputter-deposited MoS_2, it has been known that fracture and detachment of film particles can occur [1]. The earlier generation of films generally showed a columnar plate (zone 2) morphology with significant porosity [2]. There are several disadvantages to this morphology. The majority of the film is in the wrong orientation for lubrication, i.e. the basal planes are perpendicular to the substrate. In practice, the plates detach and reorient into lubricating particles. The inherent porosity of this structure promotes detachment near the bottom of the film, i.e. most of the film becomes loose particles almost immediately. Although it is now accepted that MoS_2 films lubricate by intercrystalline slip with ultimate wear of detached particles out of the contact zone [3], the generation of significant film debris early in contact has been considered undesirable, because long endurance lubrication becomes strongly dependent on the retention or recirculation of the film particles in the contact zone rather than on the gradual wearing away of the film [4,5].

Recently, films with new types of microstructure have become available which are being investigated for higher cycle precision applications, such as sensor gimbal bearings and scan mirrors [6,7]. These newer films have dense morphologies, often with basal plane orientation parallel to the substrate. Such microstructures can be prepared by adjusting the deposition conditions (pressure, deposition rate, use of ion beams) or by incorporating co-sputtered or multilayer dopants [8–13].

Ideally, these dense films lubricate by the gradual generation (wear) of fine MoS_2 particles as postulated in the model of intercrystalline slip. However, in many cases, discrete film spallation has been observed. Fig. 1 shows electron micrographs of thrust bearing raceways lubricated with MoS_2 films having zone 2 and dense MoS_2 morphologies. The raceways were disassembled after 50 000 revolutions (50 krevs). In both cases, significant film spallation was observed. Large film particles had transferred onto the originally unlubricated balls and retainers. The bearings were reassembled and the films functioned with acceptable torque for 600–2000 krevs before failure (which was defined as a tenfold rise in torque above operational values). While such particle lubrication may be adequate for torque noise tolerant applications, as in these thrust bearing tests, this process was found to increase torque noise (jitter) to unacceptable levels in tests of angular contact bearings [15].

Understanding the nature of fracture and crack propagation as a function of MoS_2 film microstructure is one of the elements required to determine optimum lubricating particle size. (Other aspects in rolling contact include, at a minimum, the effect of ball surface composition and retainer composition on MoS_2 film transfer rates from the raceways.) The brale indentation test can be used to assess toughness in MoS_2 films, within the film or along the interface. To date, the test has been successful in correlating interfacial adhesion with substrate surface treatments, including acid and base etching, ion bombardment and nitrogen implantation on steel or titanium alloys [16–19].

Limited data on the effect of MoS_2 microstructure on

Zone 2 Morphology Pure MoS₂   **Multilayer Morphology 0.9 nm Au-20%Pd/10 nm**
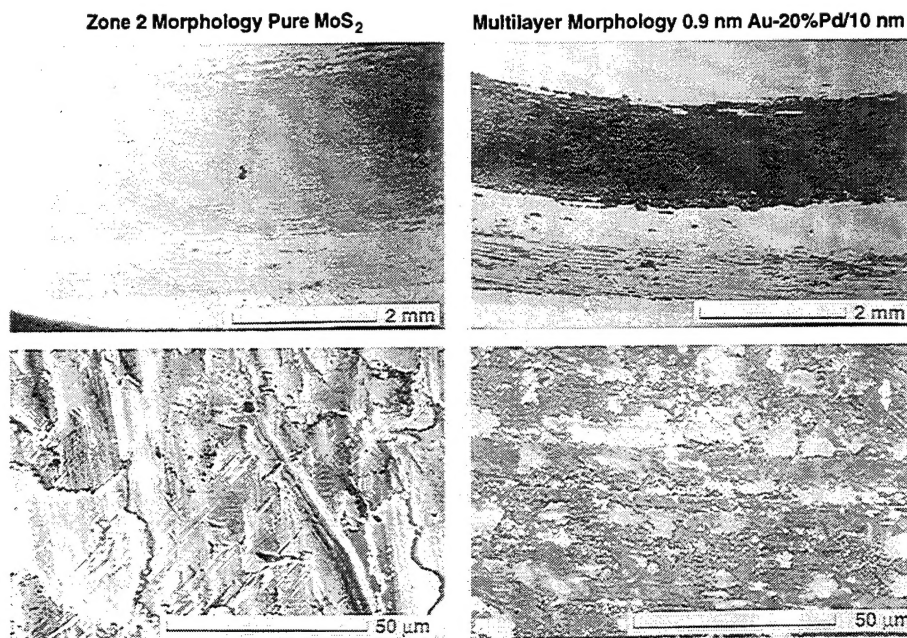

Fig. 1. Scanning electron micrographs of two 440C steel thrust bearing raceways (INA W1-1/2) disassembled after 50 krevs. The bearing raceways were lubricated with MoS₂ films: a zone 2 film (left) and a 0.9 nm Au–20%Pd/10 nm multilayer film (right). The balls and steel cages were not lubricated. The bearings had been running with adequately low, stable torque. However, significant film spallation occurred on both raceways. The bearings were reassembled and they operated with low torque for 2000 krevs and 600 krevs respectively. Original magnification: 18 × (top), 1000 × (bottom). Test conditions: 2500 rev min⁻¹; 0.5 GPa mean hertzian stress; 1 atm dry nitrogen. For further details, see Ref. [14].

indentation fracture response have been reported [5,13]. The only quantitative data reported compared zone 2 films with dense films resulting from co-sputtered water vapor [5]. In this paper, we present quantitative data on dense films as a function of metal dopants, either co-sputtered or as multilayers. The potential significance of these findings to rolling element bearings will be discussed.

2. Experimental procedures

All films were deposited onto 440C bearing steel ($R_C = 56$–58) polished down to 0.3 μm alumina. MoS₂ films having co-sputtered dopants (group I) were prepared at 2.6 Pa argon background pressure by d.c. diode sputtering using procedures reported elsewhere [9,10]. The dopants were incorporated into pressed powder targets. Four target compositions were used: MoS₂, 3%Ni–MoS₂, 9%Ni–MoS₂, 35%SbO$_x$–MoS₂. MoS₂ films having metal multilayers were also prepared by r.f. magnetron sputtering at 0.266 Pa as reported in Ref. [11]. Ni or Au–20%Pd metal layers were deposited from separate targets between the MoS₂ layers. Two groups (II and III) of films were prepared in different time periods. The group II films had the following compositions: MoS₂ (II), 0.25 nm Ni/5 nm, 0.5 nm Ni/5 nm, 0.75 nm Ni/5 nm, 1 nm Ni/5 nm, 0.7 nm Ni/10 nm and 0.9 nm Au–Pd/10 nm. (The metal thicknesses were extrapolated from the deposition rates of thicker calibration films; the multilayer periodicities were measured by X-ray diffraction by the vendor.) All of the metal-containing films had an initial metal interlayer deposited onto the substrate. Group III films had the following compositions: MoS₂ (III), 1.5 nm Au–20%Pd/10 nm and 4.5 nm Au–20%Pd/10 nm. The group III samples were originally witness plates during deposition runs to prepare films for rolling contact (i.e. ball between flats) and rolling element bearing studies as reported by Hopple et al. [15].

Indentations were made using a standard Rockwell hardness tester with a C-scale diamond stylus (having 0.2 mm radius of curvature). Three loads were used: 70, 110 and 160 kgf (these values include the minimum 10 kgf applied load of the machine, i.e. 60kgf + 10kgf, etc.). Scanning electron microscopy (SEM) was used to characterize the film morphology, thickness and delamination and fracture induced by indentation. The back-scattered electron (BSE) mode was primarily used to examine indentations. Ten measurements of the extent of delamination and/or fracture were determined for each indentation and the reported values are the mean

averages of the measurements. Three or more indent-ations per load were made on the co-sputtered films. Generally only one indentation per load could be made on the group II multilayer films, because some of the sample area had been used for sliding wear tests. The group III films were received with three or more indent-ations at each load already on them. A new indentation at each load was made for comparison.
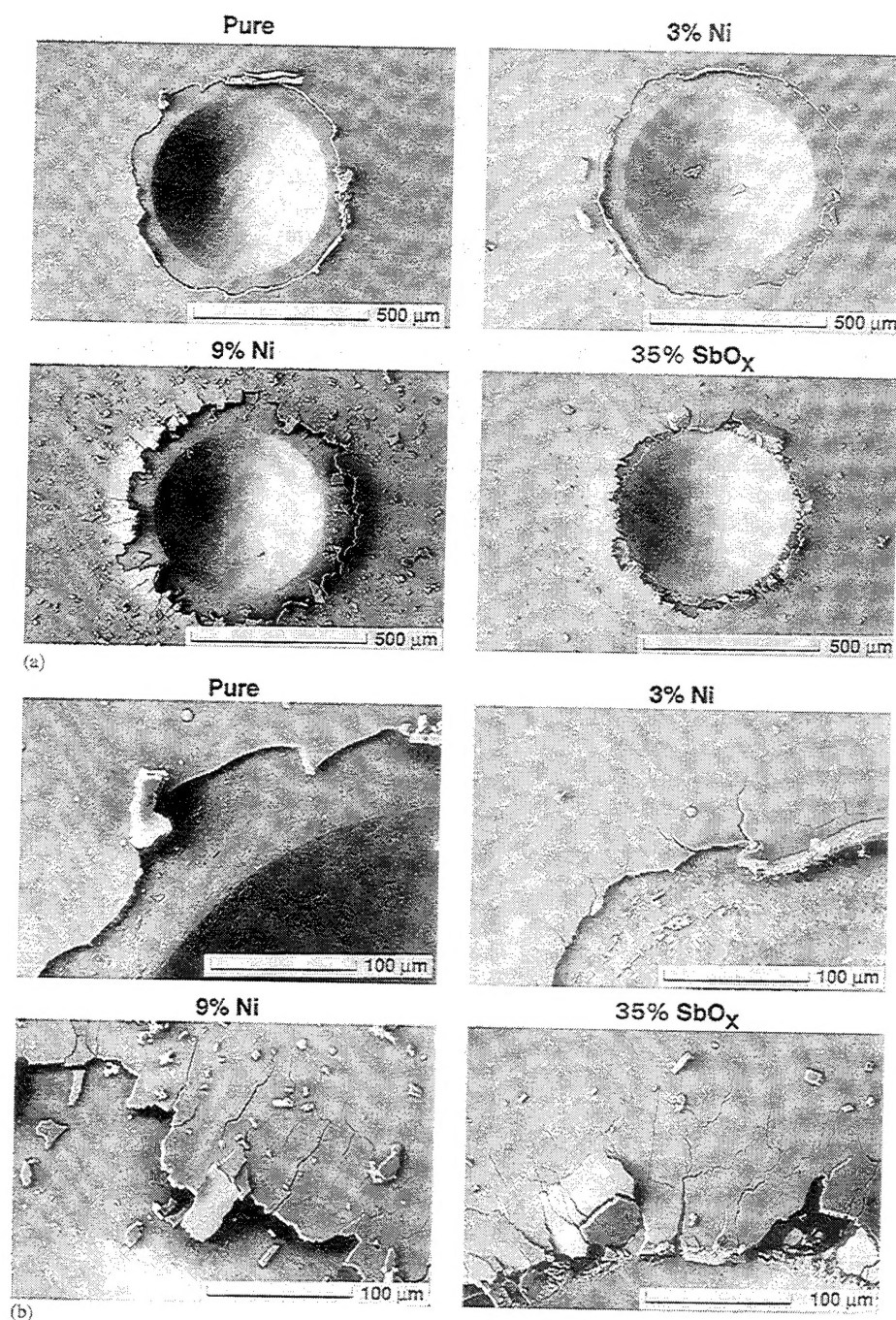

Fig. 2. (A) Scanning electron micrographs of the brale indentations of the co-sputtered films. (B) At higher magnification, radial fracture is noticeable in the films having higher concentrations of Ni or SbO$_x$. The SbO$_x$-containing film has significant branched radial fracture with little delamination.

3. Results

3.1. Morphology and thickness

The pure and 3% Ni films have columnar plate zone 2 morphologies with porosity between the plates. The 9% Ni films have a dense zone 1 morphology. The SbO_x–MoS_2 films have a very (featureless) dense morphology near the interface with a zone 1 cauliflower morphology above. The films have thicknesses of 6.3 μm, 6.8 μm, 3.2 μm and 3.9 μm respectively. The multilayer films have dense, almost featureless, morphologies with (002) basal orientation or no detected MoS_2 orientation as reported previously [13]. Film thicknesses are 1 ± 0.1 μm. The pure MoS_2 films in groups II and III prepared at 0.266 Pa have dense morphologies with mixed (002) basal and (100) and (110) edge facet orientations.

3.2. Indentation: co-sputtered films

Fig. 2 shows micrographs of the 160 kgf indentations of the co-sputtered films. The pure MoS_2 film shows simple delamination. The 3% Ni film has comparable complete delamination with some radial cracking extending beyond the delamination region. The 9% Ni film has more radial cracking, and the remnant film adjacent to the radial cracks appears delaminated (SEM at high tilt angle confirms this observation, but the exact extent of film–substrate fracture under the curled, remnant pieces is difficult to confirm). The 35%SbO_x–MoS_2 film has the least delamination, although Fig. 2 shows that significant branched, radial cracking is present. In Fig. 3, the extent of damage, i.e. fracture plus radial cracking, with and without the indentation radius is plotted as a function of load. The plotted extent of damage includes radial cracking, i.e. curled, delaminated film that has not fully detached. If pure delamination is plotted, the 9% Ni films are (erroneously) construed as showing less damage. Since the radial cracks in the SbO_x film are difficult to see in the lower magnification micrographs of Fig. 2, values based on the higher magnification micrographs are also plotted.
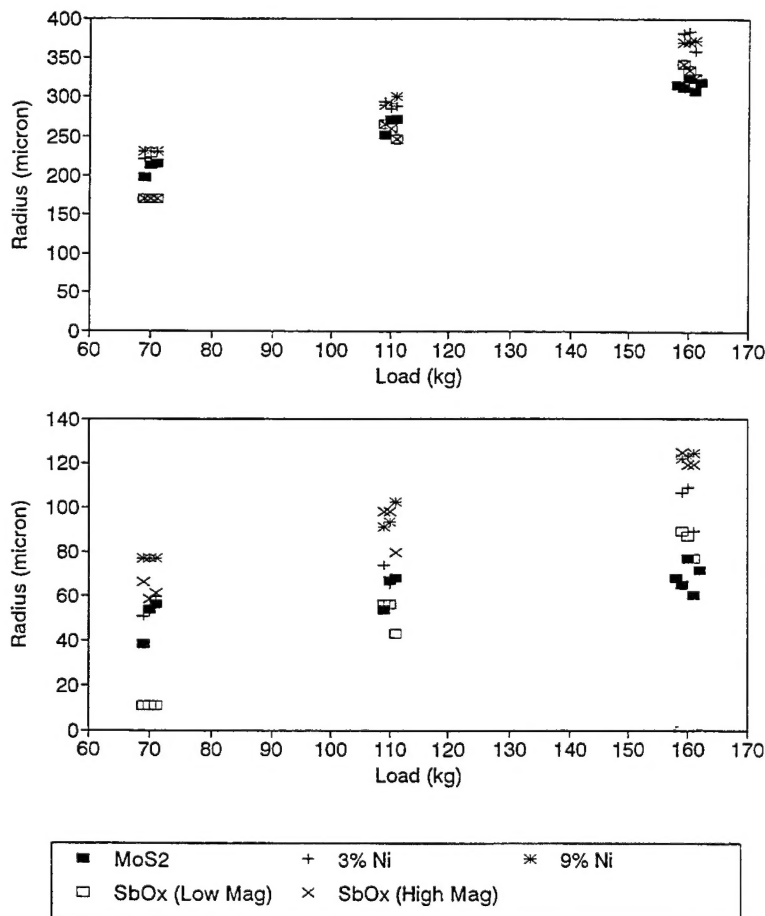

Fig. 3. Plots of the damage (delamination plus radial fracture) radii as a function of indentation load of the co-sputtered films shown in Fig. 2. Top: includes indentation radii. Bottom: indentation radii subtracted.

3.3. Indentation: multilayer films

Micrographs of the indentations of some of the group II films are shown in Fig. 4 and delamination and fracture data are plotted in Fig. 5. The pure (micro not shown) and 0.25 nm Ni/5 nm films show extensive delamination without radial cracking. Indeed, the 0.25 nm Ni/5 nm film shows more delamination than the pure film. There is an abrupt transition in fracture mode appearance between the 0.25 nm Ni/5 nm and 0.5 nm Ni/5 nm films. The latter film shows less delamination, but exhibits a network of finely spaced radial cracks, with significant branching. The 0.75 nm Ni/5 nm and 1 nm Ni/5 nm films (micros not shown) have a similar appearance to the 0.5 nm Ni/5 nm film. The 0.7 nm Ni/10 nm film shows significantly more delamination and fracture than 5 nm periodicity films with 0.5–1 nm Ni. The 0.9 nm Au–20%Pd/10 nm film shows less delamination than the 0.7 nm Ni/10 nm film.

Micrographs of the group III films are shown in Fig. 6. Although the extent of fracture is similar between the new and old sets, the newer indentations tend to show remnant delaminated film that gives some insight into crack propagation. Remnants on the older indentations may have been blown off or otherwise lost during handling/travel. As in the co-sputtered films, the inclusion of radial cracking in the estimation of the extent of damage appears to be a reasonable assessment approach.

The pure film shows more delamination than the multilayer films, and the older indentations of the pure film exhibit an extended bilayer fracture. The extent of fracture and delamination for the 1.5 nm Au–20%Pd/10 nm film is similar to the 4.5 nm Au–Pd/10 nm film. The 4.5 nm Au–20%Pd/10 nm film shows evidence of crack branching in the newer indentation. The extent of delamination and/or fracture as a function of load is plotted in Fig. 7.

4. Discussion

The indentation data show that the zone 2 films are more resistant to indentation-induced fracture propagation on a scale pertinent to spallation than the pure dense films. The zone 2 films are probably more resistant to fracture because they contain significant porosity. This porosity could reduce or relieve the build-up of stresses and/or blunt propagating crack tips. Pure, uniform, dense microstructures are susceptible to spallation. Some type of compensation is required to inhibit fracture propagation.

The data on the co-sputtered films are complicated by the fact that the 9% Ni and SbO_x films are thinner than the pure and 3% Ni films. However, delamination increases with thickness at constant applied stress for a

0.25 nm Ni/5nm   **0.5 nm Ni/5 nm**

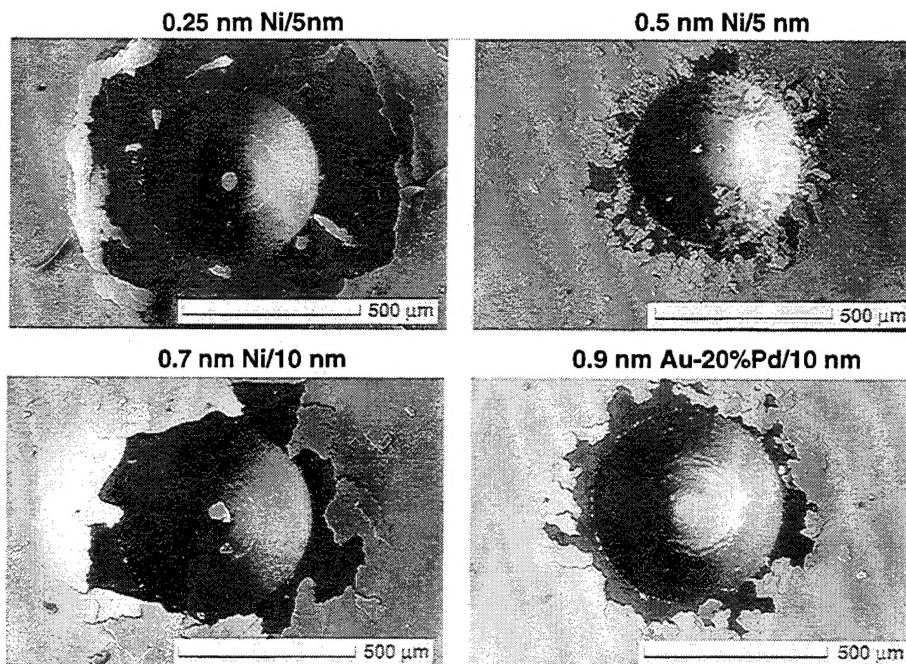**0.7 nm Ni/10 nm**   **0.9 nm Au-20%Pd/10 nm**

Fig. 4. Scanning electron micrographs of the brale indentations of some of the group II multilayer films. There is a dramatic suppression of delamination fracture in the 0.5 nm Ni/5 nm film relative to the 0.25 nm Ni/5 nm film. A fine network of branched, radial cracks is also present in the 0.5 nm Ni/5 nm film. More delamination is present in the 10 nm periodicity films.
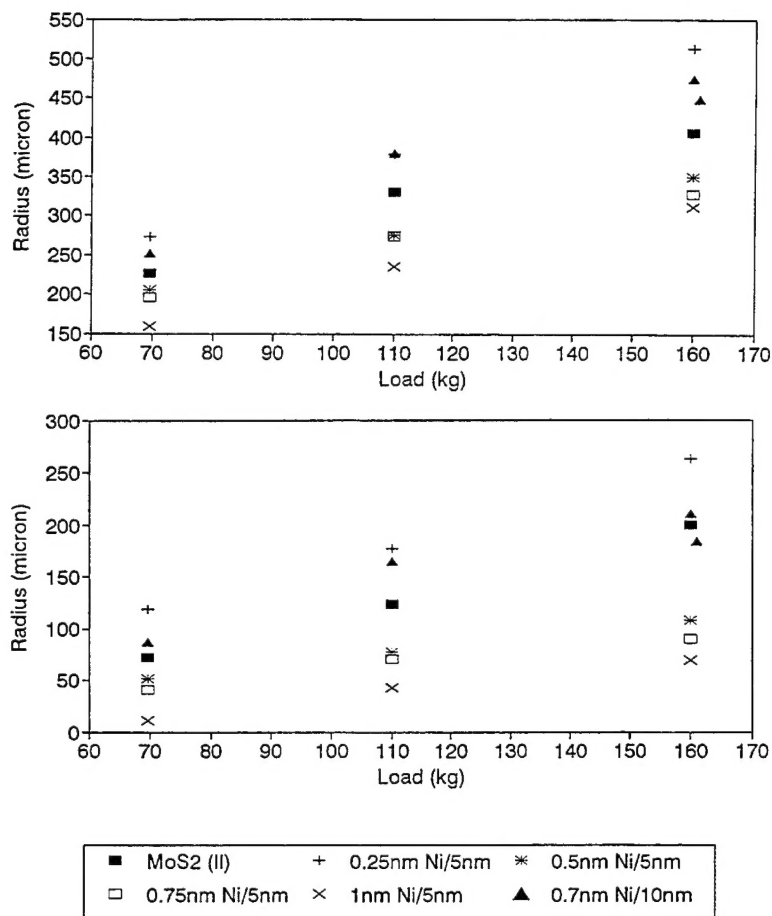
Fig. 5. Plots of the damage (delamination plus radial fracture) radii of the group II Ni multilayer films (see Fig. 4). Top: includes indentation radii. Bottom: indentation radii subtracted.

given microstructure [5]. The 9% Ni films are thinner than, but more delaminated than, the pure and 3% Ni zone 2 films. Thus co-sputtered nickel in the 9% range yields a microstructure that decreases film fracture toughness. The SbO_x data are more ambiguous. Delamination decreases relative to the other films, but there is a damage region of fine cracks comparable in area to the delaminated zone of the other films. The SbO_x films show a composite morphology, which complicates the results further. However, at these high concentrations, SbO_x appears to be a better co-sputtering additive than Ni. Considering that, with MoS₂, SbO_x is tribologically effective, it seems to be the better additive [20]. In all of the films studied, the use of a subsurface fracture detection technique, such as scanning electron acoustic microscopy [21] or X-ray methods, may help in the better quantification of the extent of film delamination of fragments that have not fully detached.

At a thickness of 1 μm, the 5 nm multilayer films show more fracture resistance than the 10 nm films. There is

a dramatic increase in fracture resistance when the metal thickness is increased from 0.25 to 0.5 nm. The fine networks of cracks suggest that the multilayers induce significant radial crack branching. Clearly, the nanostructure is changing in a manner that affects crack propagation. Although the multilayer periodicities of these films were accurately determined by X-ray diffraction, the actual film nanostructures are not known. These metal thicknesses are averages based on deposition rates. For example, it is very doubtful that the thin metal layers are continuous and we do not yet know what quantity of deposited metal is required for a continuous layer to form. At 10 nm periodicity, the limited data suggest that Au–20%Pd is more effective than Ni in inhibiting fracture. This is fortunate as friction data favor Au–20%Pd over Ni [13].

The observation that 1.5 nm periodicity Au–20%Pd films have essentially comparable fracture to 4.5 nm periodicity Au–20%Pd films is surprising, since the latter composition was developed to improve fracture response

Pure

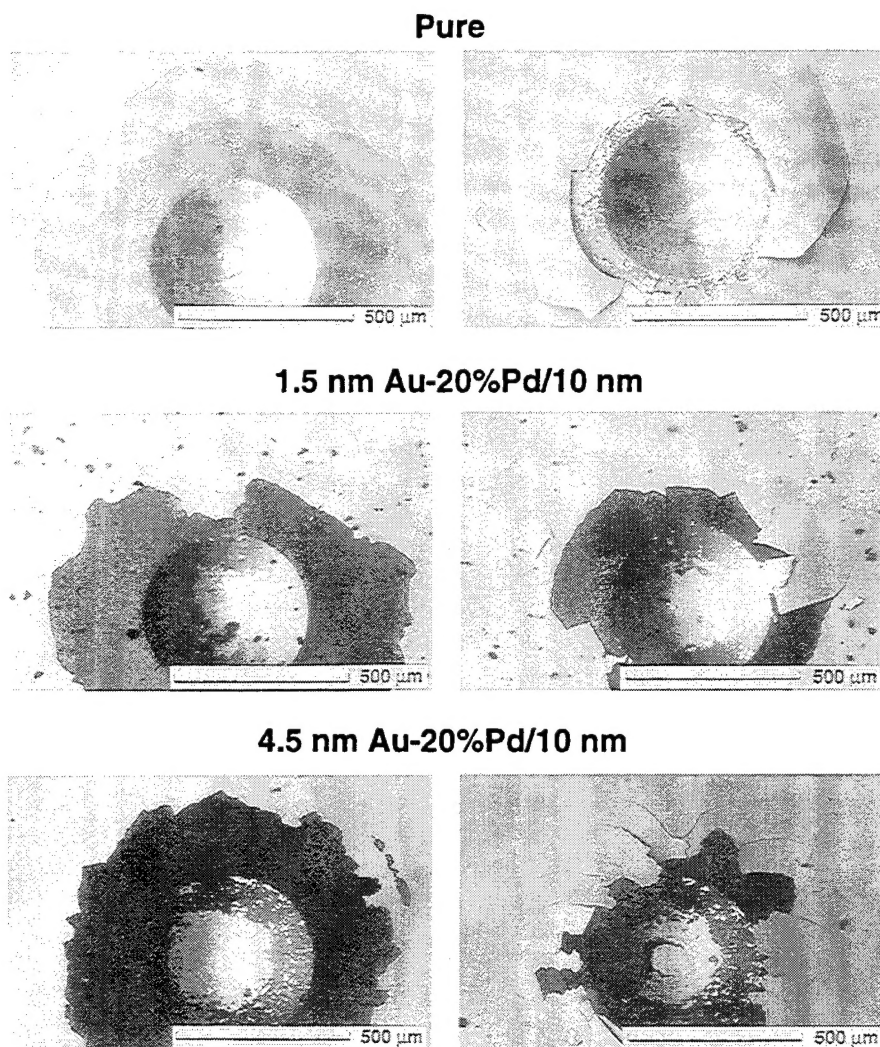## 1.5 nm Au-20%Pd/10 nm

4.5 nm Au-20%Pd/10 nm

Fig. 6. Scanning electron micrographs of the brale indentations of some of the group III multilayer films. Indentations on the left were as-received, while indentations on the right were made after receipt. The newer indentations show extensive fracture, but instructive fragments of delaminated film are still present. Unimpeded circumferential cracking is evident in the pure film, while the 4.5 nm Au–20%Pd/10 nm films show radial crack branching. (Samples courtesy of G. Hopple, Lockheed Missiles and Space Co.)

in rolling contact. However, this improved response was observed in 0.3 μm films in rolling contact [15]. Hopple [22] has found that indentation fracture of the 4.5 nm Au–20%Pd/10 nm composition is inhibited in films of 0.3 μm thickness. Interfacial stresses increase with film thickness, and increasing the multilayer metal thickness from 1.5 to 4.5 nm at 10 nm periodicity appears to be insufficient to retard fracture in films 1 μm thick. Again, these nanostructures are not well characterized in terms of the continuity of the metal layers.

Taken together, the Ni and Au–20%Pd data indicate that decreasing the multilayer periodicity is more effective than increasing the multilayer metal thickness in improving fracture toughness. This suggests that improved fracture resistance is due to some type of interfacial decohesion between the MoS₂ and metal layers, rather than to deformation within the metal layers. However, the tribological properties of the high Ni 5 nm films are very poor [13]. It would be interesting to obtain indentation and tribological data on Au–20%Pd/MoS₂ multilayer films having 5 nm periodicity at a film thickness of 1 μm.

In rolling element bearings, the torque requirements and torque noise sensitivity of the application will determine which microstructures are acceptable. In situations where torque noise is to be minimized, dense films with poor fracture resistance, such as the 9% Ni co-sputtered films, pure films prepared at low pressures and the lower
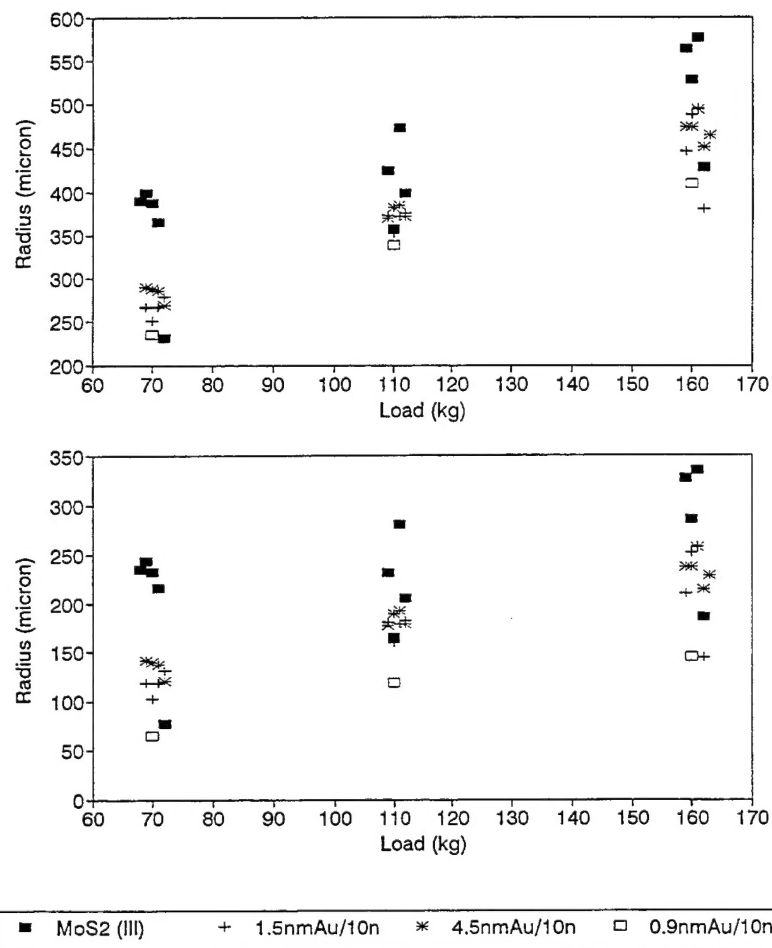
Fig. 7. Plots of the damage (delamination plus radial fracture) radii of the group II and III Au–20%Pd multilayer films (see Figs. 4 and 6). Top: includes indentation radii. Bottom: indentation radii subtracted.

metal content multilayer films would appear to be undesirable. Although the indentation tests provide insight into the tribological properties, final optimization of film nanostructure needs to be guided by rolling contact tests. In addition to jitter considerations, the need to avoid particle contamination in some applications (e.g. optics, semiconductor manufacturing) may place additional requirements on fracture resistant MoS₂ film nanostructures.

5. Conclusions

Indentation testing of sputter-deposited MoS₂ films containing additives has identified different fracture responses for specific morphologies. Films showing porous zone 2 columnar plate morphologies generally exhibit less delamination than films with dense mor-

phologies. Films containing 9% co-sputtered Ni with dense zone 1 morphologies exhibit more delamination than pure or 3% Ni zone 2 films. The presence of 35% SbO$_x$ in zone 1 films inhibits delamination, although a network of branched radial and circumferential cracks develops. For multilayer films with a total thickness of 1 μm, significant fracture is observed when the extrapolated metal thickness is less than 0.5 nm, suggesting that a critical difference in nanostructure is present between films with lower amounts of metal and those with 0.5 nm or more of metal. The presence of multilayers of sufficient thickness causes radial crack branching. Decreasing the multilayer periodic spacing (i.e. increasing the number of multilayers) inhibits delamination more effectively than increasing the metal thickness above a critical value. Fracture toughening appears to stem from interfacial decohesion. Although more experiments are needed, Au–20%Pd appears to

be more effective as a fracture inhibitor than Ni in multilayer films.

References

[1] T. Spalvins, *ASLE Trans.*, *14* (1971) 267; *17* (1973) 1; *Thin Solid Films*, *96* (1982) 17.
[2] M.R. Hilton and P.D. Fleischauer, *Mater. Res. Soc. Symp. Proc.*, *140* (1989) 227.
[3] P.D. Fleischauer and R. Bauer, *Tribol. Trans.*, *31* (2) (1988) 239.
[4] P.D. Fleischauer, M.R. Hilton and R. Bauer, Effects of microstructure and adhesion on performance of sputter-deposited MoS$_2$ solid lubricant coatings, in D. Dowson, C.M. Taylor and M. Godet (eds.), *Mechanics of Coatings*, Leeds–Lyon 16, Tribology Series 17, Elsevier, Amsterdam, 1990, p. 121.
[5] M.R. Hilton, R. Bauer and P.D. Fleischauer, *Thin Solid Films*, *188* (1990) 219.
[6] M.R. Hilton and P.D. Fleischauer, *Surf. Coat. Technol. 54/55* (1992) 435.
[7] S.H. Loewenthal, R.G. Chou, G.B. Hopple and W.L. Wenger, Evaluation of ion-sputtered molybdenum disulfide bearings for spacecraft gimbals, *Tribol. Trans.*, *37* (3) (1994) 505.
[8] C. Muller, C. Menoud, M. Maillat and H.E. Hintermann, *Surf. Coat. Technol.*, *36* (1988) 351.
[9] A. Aubert, J.Ph. Nabot, J. Etnoult and Ph. Renoux, *Surf. Coat. Technol.*, *41* (1990) 127.
[10] R.N. Bolster, I.L. Singer, J.C. Wegand, S. Fayeulle and C.R. Gossett, *Surf. Coat. Technol.*, *46* (1990) 207.
[11] B.C. Stupp, *Thin Solid Films*, *84* (1981) 257.
[12] B.C. Stupp, *Proc. Third Int. Conf. on Solid Lubrication*, *ASLE SP-14*, Society of Tribologists and Lubrication Engineers, 1984, p. 217.
[13] M.R. Hilton, R. Bauer, S.V. Didziulis, M.T. Dugger, J. Keem and J. Scholhamer, *Surf. Coat. Technol.*, *53* (1992) 13.
[14] S.V. Didziulis, M.R. Hilton, R. Bauer and P.D. Fleischauer, Thrust bearing wear life and torque tests of sputter-deposited MoS$_2$ films, *TOR-92(2064)-1*, The Aerospace Corporation, October, 1992.
[15] G.B. Hopple, J.E. Keem and S.H. Loewenthal, *Wear*, *162–164* (1993) 919.
[16] M.R. Hilton, R. Bauer, S.V. Didziulis and P.D. Fleischauer, *Thin Solid Films*, *00* (1991) 49.
[17] S.V. Didziulis, M.R. Hilton and P.D. Fleischauer, The influence of steel surface chemistry on the bonding of lubricant surfaces, in Y.-W. Chung, A.M. Homola and G. Bryan Street (eds.), *Surface Science Investigations in Tribology*, ACS Symp. Ser. 485, 1992, pp. 43–57.
[18] X. Zhang, P. Zhang, H. Liu, W. Zhao and S. Xu, *Thin Solid Films*, *229* (1993) 58.
[19] F.M. Kustas and M.S. Misra, Friction and wear of titanium alloys, in P.J. Blau (ed.), *ASM Handbook*, Vol. 18, Friction, Lubrication, and Wear Technology, ASM International, Materials Park, OH, 1992, p. 778, and references cited therein.
[20] J.S. Zabinski, M.S. Donley and N.T. MeDevitt, *Wear*, *165* (1993) 103, and references cited therein.
[21] T. Page, *Inst. Phys. Conf. Ser.*, *138* (7) (1993) 295, and references cited therein.
[22] G. Hopple, Lockheed Missiles and Space Co., Sunnyvale, CA, personal communication, 1994.

TECHNOLOGY OPERATIONS

The Aerospace Corporation functions as an "architect-engineer" for national security programs, specializing in advanced military space systems. The Corporation's Technology Operations supports the effective and timely development and operation of national security systems through scientific research and the application of advanced technology. Vital to the success of the Corporation is the technical staff's wide-ranging expertise and its ability to stay abreast of new technological developments and program support issues associated with rapidly evolving space systems. Contributing capabilities are provided by these individual Technology Centers:

Electronics Technology Center: Microelectronics, VLSI reliability, failure analysis, solid-state device physics, compound semiconductors, radiation effects, infrared and CCD detector devices, Micro-Electro-Mechanical Systems (MEMS), and data storage and display technologies; lasers and electro-optics, solid state laser design, micro-optics, optical communications, and fiber optic sensors; atomic frequency standards, applied laser spectroscopy, laser chemistry, atmospheric propagation and beam control, LIDAR/LADAR remote sensing; solar cell and array testing and evaluation, battery electrochemistry, battery testing and evaluation.

Mechanics and Materials Technology Center: Evaluation and characterization of new materials: metals, alloys, ceramics, polymers and composites; development and analysis of advanced materials processing and deposition techniques; nondestructive evaluation, component failure analysis and reliability; fracture mechanics and stress corrosion; analysis and evaluation of materials at cryogenic and elevated temperatures; launch vehicle fluid mechanics, heat transfer and flight dynamics; aerothermodynamics; chemical and electric propulsion; environmental chemistry; combustion processes; spacecraft structural mechanics, space environment effects on materials, hardening and vulnerability assessment; contamination, thermal and structural control; lubrication and surface phenomena; microengineering technology and microinstrument development.

Space and Environment Technology Center: Magnetospheric, auroral and cosmic ray physics, wave-particle interactions, magnetospheric plasma waves; atmospheric and ionospheric physics, density and composition of the upper atmosphere, remote sensing using atmospheric radiation; solar physics, infrared astronomy, infrared signature analysis; effects of solar activity, magnetic storms and nuclear explosions on the earth's atmosphere, ionosphere and magnetosphere; effects of electromagnetic and particulate radiations on space systems; space instrumentation; propellant chemistry, chemical dynamics, environmental chemistry, trace detection; atmospheric chemical reactions, atmospheric optics, light scattering, state-specific chemical reactions and radiative signatures of missile plumes, and sensor out-of-field-of-view rejection.